



An adaptive deep learning approach for identification of crop-types from remote sensing images

Shilpa Vatkar¹ · Sujata Kulkarni¹

Received: 18 November 2024 / Accepted: 20 May 2025

© The Author(s), under exclusive licence to Springer-Verlag GmbH Germany, part of Springer Nature 2025

Abstract

Accurate crop-type maps that are updated regularly are necessary for various agricultural monitoring and decision-making purposes. Obtaining crop-type maps early in the current growing season is highly advantageous for agricultural decision-making and management. Due to the abundance of high-resolution remote sensing data with precise spatial and temporal details, the frequency of data collection from various sources is anticipated to rise. The augmentation of data gathering will yield a larger volume of information available in the initial phases of the season. This study proposed an Adaptive Convolutional Neural Network with Incremental Training (ACNN-IT) method based on the CNN model. ACNN-IT is primarily intended to explore the potential of integrating diverse data sources for real-time crop-type identification. Given the periodic production of Sentinel remote sensing data, an adaptive strategy for early crop-type detection is necessary. Consequently, the incremental training-based CNN model is developed for autonomous feature extraction and classification. The proposed model comprises pre-processing, feature extraction, and classification. An iterative training method is utilized to familiarize the network with adaptive sentiment data and ascertain the ideal detection rate for each crop variety throughout the early growth season. An examination of the ACNN-IT model is conducted using remote sensing data collected from Sentinel-1 A and Sentinel-2 satellites. ACNN-IT strategy was validated using support vector machine (SVM), random forest (RF), and SoftMax classifiers. Simulation results revealed that the proposed model has improved the overall crop type detection accuracy by 3.56% with reduced computational burden by 7.23% compared to the state-of-the-art.

Keywords Crop-type detection · Convolutional neural network · Incremental training · Remote sensing · Sentinel images

1 Introduction

India's rapid agricultural technological improvement has resulted in intelligent agriculture. Broad, comprehensive agriculture monitoring is needed. The impartiality and cost-effectiveness of remote sensing in agriculture are driving its growth [1–3]. Remote sensing calculates yield, identifies crop kinds, inverts soil moisture, and tracks growth and phenology [4–7]. National government organizations must designate crop sorts to understand crop production

for agricultural management. Visual interpretation [8] and computer-assisted categorization [9] are prominent remote-sensing crop-type identification approaches. Visual crop-type identification has been successful. However, weather impacts optical remote sensing [10, 11]. Clouds and rain are typical during crop growth. Good images are hard to acquire, affecting crop type identification precision and speed. Microwave remote sensing has become popular [12]. In every condition, Synthetic aperture radar (SAR) data may be acquired continuously. Leaf, stem, and branch attributes can be presented with crop surface properties [13]. Sentinel-1 A pictures' improved geographical and temporal resolution assures data dependability and proposes crop-type identification and categorization. Therefore, Sentinel-1 A may be the main data source for this investigation. Sentinel-2 also identifies crops.

Maps of crop kinds aid agricultural management and administration. Crop rotation, production projections, and

✉ Shilpa Vatkar
shilpa.kale@spit.ac.in

Sujata Kulkarni
sujata_kulkarni@spit.ac.in

¹ Department of Elec.& Telecommunication, Sardar Patel Institute of Technology, Andheri, Mumbai, India

agricultural catastrophe assessment require seasonal crop data [14]. This is crucial for food security. Excellent spatial and temporal resolution Satellite SAR and optical remote-sensing can identify crop types early. European Copernicus employs Sentinel-1 A/B (S1) and S2 satellites. In addition to SAR and optical (multispectral) imaging, S1 and S2 may give 10-meter spatial and 5 or 6-day temporal resolutions. Integrating the two data sets enhances early crop-type identification.

- (1) The comprehensive crop phenology data obtained from dense time series can be employed to differentiate between crop varieties that have identical spectra [15].
- (2) Multisource remote sensing data, unlike single-source data, provide a higher temporal frequency of data collection, hence immediately improving timeliness.
- (3) Different sensors demonstrate varying sensitivities to crop factors; optical data can assess the chemical constituents of crops, including chlorophyll and water [16].

Increased crop structure (porosity, height, and coverage) and field conditions (moisture content) sensitivity in SAR data [17]. In-season mapping makes S1 and S2 data integration harder. Random forest (RF) and support vector machine (SVM) may struggle with sequential links in time series imaging. This might lose vital crop-type detection data [18]. Recent improvements in machine learning (ML) make deep learning (DL) intriguing for remote sensing data extraction [19]. In many respects, deep learning has this capacity. Deep learning excels in temporal data extraction [20]. CNNs and RNNs are well-known neural networks. GRU and LSTM networks can substitute RNNs for gradient fading or explosion in long-time series data. The majority of these models have been evaluated in crop-type mapping utilizing microwave data [21], vegetation index (or optical data), or CNN-LSTM hybrid architecture to transfer SAR data to NDVI [22]. These methods are inadequate for multisource data because single-source time series have consistent sequence lengths and spectral band time intervals. Varied sources produce time series with varied sequence lengths and intervals. Unfortunately, present systems lack correct coefficient estimate algorithms that use sentinel information.

Recent algorithms like Gated Recurrent Unit (GRN) and CNN merge S1 and S2 images to enhance land cover categorization, however they cannot distinguish crop variety in season. CNNs have fewer parameters than RNNs relative to the time series duration. Deep learning architectures use time series to find the ideal date, making training time-consuming with many parameters. Current deep learning systems are too computationally intensive to identify crop kinds from sentinel data early. The inability to adapt to time series data for crop type detection hinders existing

techniques. Adaptive Convolutional Neural Network with Incremental Training (ACNN-IT) is a new deep learning model that addresses these concerns. The list of important contributions emphasizes the manuscript's uniqueness.

- The ACNN-IT model initially introduces the pre-processing phase, during which the input sentinel picture undergoes enhancement for quality improvement using appropriate filtering and smoothing functions.
- The pre-processing phase is enhanced by a hybrid method for coefficient estimation that employs NDVI and backscattering technique to optimize the effectiveness of Sentinel images for precise crop type identification.
- The subsequent phase of ACNN-IT involves DL-based feature extraction. The adaptive and lightweight CNN layers are engineered to facilitate the gradual learning of time-series sentinel data, allowing for enhanced utilization of information in the early season and augmenting the sensitivities of optical and radar data across many parameters.
- This is the final contribution, which consisted of a study of the ACNN-IT model using remote sensing data received from the Sentinel-1 A and Sentinel-2 satellites. Classifiers such as SVM, RF, and SoftMax are utilized to validate the ACNN-IT approach.

This section provides a summary of the remaining portions of the manuscript it contains. In Sect. 2, we will examine the approaches that are currently in use. Section 3 will describe the research location and dataset. Section 4 will provide specifics regarding the ACNN-IT methodology and its design. Section 5 will assess the outcomes of the experiments, and Sect. 6 will conclude the study.

2 Related works

Satellite-hosted or airborne sensors on drones, other lightweight aircraft, or UAVs provide remote sensing data. Non-satellite techniques are expensive and not covered. The study employs sentinel 1 A/2 satellite data. Meteorology, agriculture, and geology use satellite data. Advanced computer vision and Artificial Intelligence (AI) algorithms have been used for a decade to analyze soil moisture and identify crop types using sentinel photos in agriculture. Recent advances in Deep Learning (DL) algorithms for autonomous sentinel picture processing have increased efficiency. First, several DL-based sentinel remote sensing image analyses are examined, followed by in-season crop-type detection from sentinel images.

2.1 A. DL-based Sentinel data analysis in agriculture

Computer vision and AI are used to study agricultural soil moisture using sentinel photos. With these images, crop types are identified and included throughout the procedure. This section examined soil moisture measurement using sentinel photography. In [23], a CNN architecture was developed using Sentinel-1 pictures to predict agricultural soil moisture. Sentinel-1's dual-polarization synthetic aperture radar provided us with data. The CNN architecture has six convolutional layers, one flattening layer, one max-pooling layer, and one fully connected layer. Sentinel-1 radar and Sentinel-2 optical satellite data were used to measure soil moisture [24] after removing the plant influence with a water cloud model, a standard model was used to measure soil moisture. SVR and GRNN models were then used to assess how remote sensing characteristics affected soil moisture. The researchers investigated whether it would be possible to use publicly available Sentinel-1 and Sentinel-2 earth observation data to simultaneously estimate soil moisture content (SMC) using a cycle-consistent adversarial network (cycleGAN) to compensate for time-series data gaps [25]. A unique deep-learning architecture is proposed in [26]. The vegetation index was used to predict soil moisture from satellite images in this design. U-Net semantic segmentation and sequence-to-sequence layers were used to gather pixel-wise satellite image data and SMC spatial correlation. Section [27] uses deep learning to estimate daily soil moisture levels. Climate, radar, soil, and topography time series data are used in this model. In addition, this model incorporates topographical data. The model was trained using static and dynamic soil moisture retrieval characteristics. A model using an ANN was created in [28]. This model forecasts surface soil moisture using satellite data in the massive Himalayan Foreland Kosi River alluvial fan. Surface soil moisture is predicted by this model's feedforward neural network. Graphical indicators and linear data fusion were used to analyze Sentinel-1, Sentinel-2, and Shuttle Radar Topographic Mission satellite products, identifying nine characteristics. SMC was retrieved using deep learning [29]. The dataset includes ground truth, radar incidence angle, and SAR backscattering data. This study examined five machine-learning prediction algorithms to determine their soil moisture accuracy. The article [30] described a novel soil moisture recovery method. Many vegetation indexes were created. To make modifications, the Water Cloud Model (WCM) was revised. Due to vegetation impacts, this was done. The hybrid model using Bi-GRU and Deep Max Out Network (DMN) simplified soil moisture retrieval. Improvements in score-level fusion enabled decisive results. In [31], a DL algorithm predicted

upper 5 cm soil volumetric moisture content. The model has a 320-meter imaginary resolution. The results showed that machine learning can smoothly integrate several modalities and produce high-resolution, location-independent models. In [32], a new approach was designed using Sentinel-2 data and a convolutional neural network to calculate soil moisture in vegetated areas. A CNN design was created to maximize prediction accuracy. One pooling layer, sixteen convolutional layers, and two fully connected layers comprised this architecture. In [33], cross-resolution transfer learning was pioneered for crop-type mapping. This technique assumes models with varied spatial resolutions have the same architectural frameworks and trainable features.

2.2 B. Crop-type identification using Sentinel data

In [34], different unsupervised clustering methods were used to detect distant photo cropping types. An experimental method was used to study the relationship between clustering algorithms and distance measures, which is critical to their performance. This study included over twenty datasets from five crop combinations. In [35], a novel crop-type detection approach was presented. For crop-type recognition, the convolutional autoencoder neural network (C-AENN) was created. Maximizing optimum multi-temporal feature combinations was its main goal. The technology was tested against standard machine learning methods to determine its efficacy. Data source integration was examined using Dual-1DCNN [36]. This work's CNN paradigm underpinned this method. Additionally, incremental training was used to expand the network on each data-collecting day and determine the best detection date for early-season crop kinds. In a case study in Hengshui City, China, 2019 S1 and S2 time series data were used. A novel technique for early crop mapping across the CONUS was reported in [37]. This technique uses NDVI and EVI data for dynamic ecoregion clustering. Both of these indicators quantify vegetation change over time. In [38], a comprehensive review examined the history and progress of crop mapping using remote sensing. This publication also reviews the latest crop mapping scientific discoveries using machine learning and deep learning models. The study [39] built U-Net, a fully convolutional encoder-decoder architecture for semantic segmentation. Due to hard conditions, smallholder farms grow several crops, hence this architecture distinguishes them. This was considered, unlike traditional machine learning methods. Few-shot learning (FSL) has achieved this in natural picture computer vision. Crop mapping using time series data has not been extensively studied [40]. This shortcoming was addressed using eight FSL approaches to distinguish unusual crops from France's research locations and a broad diversity of crops from Ghana's agricultural landscape. One

of the best spatially explicit active learning techniques is described in [41]. This approach uses the semi-variogram to remove duplicate data near each other geographically. Random forest analysis was used to evaluate two study locations in Belgium and the Netherlands using Sentinel-2 satellite images. A new virtual training label creation method was developed in [42]. The training samples of each crop were separated using self-organizing maps, and pixels that were not identified were tagged based on distance. This procedure was used. CNN initially planned to categorize Sentinel-clipped photographs. A temporal series of Sentinel-2 photos was used to construct a transfer learning crop classification method [43]. These photos were annotated for Vojvodina (Serbia) and Brittany. This type of crop classification was used. Google Earth Engine's high-resolution Sentinel-2 images were used to map Bengbu, China, in [44]. This mapping showed paddy rice and winter wheat output. Several deep-learning systems have mapped crop kinds. In [45], a deep learning architecture called XcelNet17 was introduced for crop photo categorization in remote sensing. XcelNet17, which consists of fourteen convolutional layers and three fully linked layers, outperformed several benchmark designs described in the literature in terms of classification accuracy. A unique boundary-enhanced dual-stream network (BEDSN) was developed in [46], incorporating an edge detection branch stream (EDBS) with a composite loss function to mitigate boundary loss in the semantic segmentation branch stream. Additionally, methods in [47–51] were proposed for automatic crop-type classification from the remote sensing images.

2.3 C. motivation

Recently developed agricultural methods include soil moisture measurement and crop-type classification or identification using remote sensing photography. Deep learning-based soil moisture analysis algorithms [23–33] using Sentinel images cannot directly identify crop types, thus, particular mechanisms are needed for in-season crop-type classification. DL and ML algorithms in [34–51] are traditional and fail to handle classification errors and computational efforts. The improper computation of Sentinel coefficients

in current crop-type mapping algorithms lowers identification rates. DL-based approaches cannot capitalize on early season data for crop-type identification due to sluggish time-series sentinel data learning. These issues lead us to develop ACNN-IT, a DL-based solution for sentinel picture crop-type recognition. ACNN-IT's main contributions have been discussed, addressing research needs.

3 Research region and data collection

3.1 Study area

Maharashtra produces a lot of India's food. Pune, a city in Maharashtra, is 800 m (2,625 feet) above sea level and covers 518 square kilometers. Pune is located at 18 degrees 32 min north and 73 degrees 51 min east. The city covers 15.642 square kilometers, while the municipal corporation serves 518 square kilometers. Pune experiences 167.11 rainy days per year, or 45.78%. Annual rainfall in Pune is calculated at 111.34 millimeters. Wheat and maize constitute the foundation of this region's agricultural rotation strategy. Cotton, the common yam rhizome, fruit trees, and vegetables are the main crops in this region. Also grown are veggies. Summer maize is grown after winter wheat and ends in September, while winter wheat is grown from October to June. Cotton grows from late March to late October, whereas common yam rhizome grows from early March to late October. Cotton grows from July to October. Fruit trees often exhibit everlasting growth patterns. This study found that summer maize, cotton, and common yam rhizome have three phases: seeding, development, and maturity.

3.2 Sentinel data

Sentinel 1 A and Sentinel 2 satellites initially provided ground truth data in the research zone. These satellites were investigated. This table describes Sentinel 1 A and Sentinel 2 data-collection satellites. Preprocessed satellite data is useful for distant intelligence photos. The ESA prepared Sentinel-1 A data. Sentinel Application Platform was used. The procedure involves these steps: Orbit file utilization, thermal noise reduction, calibration, mosaicking, speckle noise filtering, range-Doppler terrain correction, linear to dB backscatter coefficient conversion, and study region extraction are included. Sentinel 2 used atmospheric calibration, cloud blocking, resampling, and gap filling (Table 1).

3.3 Data sampling

We visited the local Department of Agriculture and Rural Affairs to understand the crop planting structure and crop

Table 1 Sentinel 1 A and 2 parameters

| Product | Sentinel-1 A/B and Sentinel 2 |
|--------------------|-------------------------------|
| Type of Product | GRD-HD |
| Acquisition mode | IW |
| Band | C band |
| Polarization | VV+VH, VV, HH, and Dual VV |
| Image size | 1024×677 |
| Frequency | 5.405 GHz |
| Spatial Resolution | 5×20 m |
| Orbits | Ascending and Descending |

Table 2 Statistics of data collected

| Class | 1 | 2 | 3 | 4 | 5 | Total |
|-------------------------|--------|--------|--------|-------------|--------|---------------|
| Crop Type | Forest | Corn | Cotton | Fruit trees | CYR | |
| No. of Parcels | 25 | 25 | 17 | 27 | 32 | 126 |
| Area (Km ²) | 2.78 | 2.93 | 4.72 | 4.89 | 5.98 | |
| Training samples | 9513 | 11,124 | 8140 | 12,587 | 15,672 | 57,036 |
| Testing samples | 4077 | 4768 | 3488 | 5395 | 6717 | 24,445 |
| Total samples | 13,590 | 15,892 | 11,628 | 17,982 | 22,389 | 81,481 |

**Fig. 1** Types crops investigated

distribution in the research region. This was done by visiting the department. A field study collected and recorded sample data from research zone crops from March to October 2022. The circumstance was complicated, thus larger samples were taken. A Global Positioning System (GPS) was utilized to find the package's four corners and verify ground data. Table 2 displays all Sentinel 1 A and 2 spacecraft data statistics. Measurements were taken by these satellites. From the possibilities, 126 parcels were chosen as examples. The parcels have 32 common yam rhizomes (CYR), 25 croplands, 25 summer corn, 17 cottons, 27 fruit trees, and 25 cotton. This project consumed 228.219 pixels. For this study, 70% of the samples were randomly selected as training samples. The remaining 30% were test samples. Table 2 lists population sample characteristics. Table 2 shows that 81,481 samples were prepared for a future crop-type identification model trial. The samples are separated into five groups with varied crops based on training and testing. Each crop sample from this experiment is shown in Fig. 1.

4 ACNN-IT methodology

This section describes ACNN-IT for early in-season crop type identification utilizing a time series sentinel dataset. An illustration of the proposed model is in Fig. 1. This paradigm involves data collection, pre-processing, CNNs, and classification. The ACNN-IT paradigm's pre-processing step differs from the data-collection stage. This phase uses computer vision methods to improve Sentinel photo quality and calculate coefficients for feature representation. In the second step of the ACNN-IT paradigm, the ACNN independently adapts to learn features from sentinel pictures. Adaptable convolutional neural networks (ACNN) retrieve properties from new sentinel time-series data. An incremental learning strategy was used to build the ACNN architecture. Incremental learning lets artificial neural networks learn without retraining. Figure 1's CNN layers enable incremental learning. Dynamic or shifting situations benefit from this strategy. It is recommended that CNNs have four

Fig. 2 Architecture of automatic crop-type identification from Sentinel data

layers: three convolutional processing and one flattening. Each convolutional layer has convolution, batch normalization (BN), and leaky ReLU activation. For effective feature extraction, 64, 128, and 64 kernel filters are used. The established classification phase includes L1 regularization, an FCL, a SoftMax layer, and crop-type identification (Fig. 2).

4.1 A. Pre-processing

4.1.1 Pre-processing

During pre-processing, the input remote sensing color picture I undergoes preparation before automated feature extraction. Before the implementation of pre-processing procedures, each input picture is resized to the typical dimensions of 512×512 . The input picture undergoes first pre-processing with the use of median filtering on each 2D color channel. Among several filtering techniques, median filtering is more effective in this study for enhancing the quality of the input RGB SAR picture. The median filter guarantees that the resultant pixel value is an authentic value from the surrounding area, so averting the generation of fake values when the filter traverses an edge. The median filter surpasses the mean filter in preserving sharp edges. Equation (1) illustrates the application of median filtering on each two-dimensional channel.

$$m^i = \sum_{i=1}^n \text{median}(I(:, :, i)) \quad (1)$$

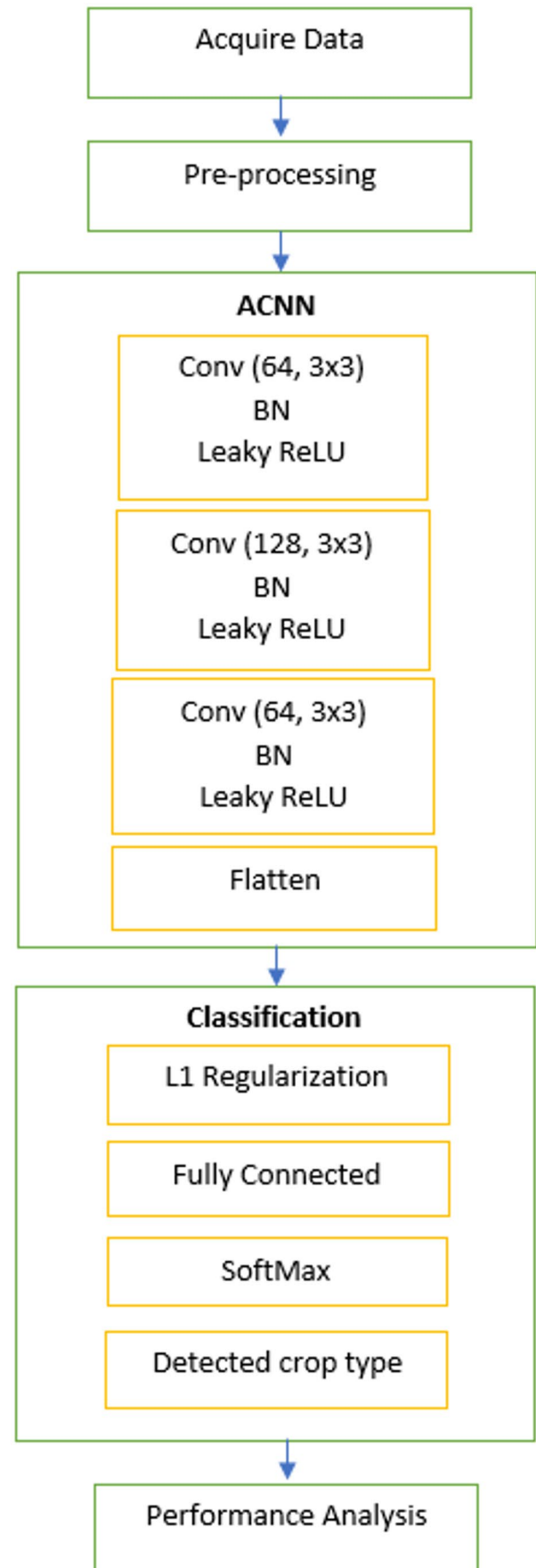
where, n represents the total number of channels which is 3 (R, G, and B), m^i represents the i^{th} filtered 2D SAR image. Subsequently, each processed image is combined to make the final filtered RGB Sentinel-1 image I^f . During pre-processing, the backscattering coefficient is calculated to determine the extra crop evaluation data in conjunction with the vegetation index NDVI. The filtered SAR image comprises many bands including R, G, and near-infrared (NIR). The NDVI and backscattering coefficient is calculated using these bands. Equations (2), (3), and (4) are used to calculate the bands G, R and NIR.

$$G = \text{double}(I^f(:, :, 1)) \quad (2)$$

$$R = \text{double}(I^f(:, :, 2)) \quad (3)$$

$$NIR = \text{double}(I^f(:, :, 3)) \quad (4)$$

We extract certain bands, such as visible Near-Infrared (NIR) and visible Red (R) bands, from the corrected Sentinel-1



SAR image to calculate NDVI (I^N) for input image I^f . NDVI is calculated using Eq. (5).

$$I^N = \frac{(NIR - R)}{(NIR + R)} \quad (5)$$

Similarly, the backscattering coefficients I^B are computed using Eq. (6).

$$I^B = add\left(\frac{(G - NIR)}{(G + NIR)}, I^N\right) \quad (6)$$

Figure 3 shows the detailed illustrations of the above steps for a sample input image. The input sentinel image is acquired which is further filtered using median filtering, and then visible red, NIR, and green bands are extracted. The estimated picture is the result derived from Eq. (6) utilizing NDVI with backscattering coefficient estimation. It enhances the processing of sentinel images for precise crop-type identification.

4.2 B. ACNN

Figure 1 shows the architecture of ACNN layers for automatic feature learning with an incremental training approach. The proposed ACNN model is trained incrementally to

acquire the newly received time-series sentinel data. A CNN may undergo incremental training. The feature engineering layers seen in Fig. 1 are constructed with the incremental learning technique known as Learn++. The Learn++ and AdaBoost algorithms [52] are originally employed for the supervised learning of neural networks. We provide an incremental learning method for CNN, inspired by the AdaBoost and Learn++ algorithms. This approach enables the integration of novel, previously unobserved sentinel data without necessitating the retraining of the whole network architecture. It employs an ensemble of modified CNN layers linked to several classifiers by producing numerous hypotheses. The modified CNN architecture has three convolutional layers and one flattening layer. Each convolutional layer comprises a 2D convolution operation with varying kernel sizes, batch normalization (BN), and a leaky ReLU activation function. Furthermore, it is prevalent to include BN in CNN designs to enhance their generalization capacity and mitigate overfitting. In classification tasks, CNNs typically comprise various combinations of L1 regularization, fully connected layers, and a SoftMax logistic regression layer, which serves as a classifier producing predicted probabilities for all object categories within the input data. The layers of the proposed ACNN model are specified as follows. The automatic feature extraction approach commences by employing the input from the pre-processing

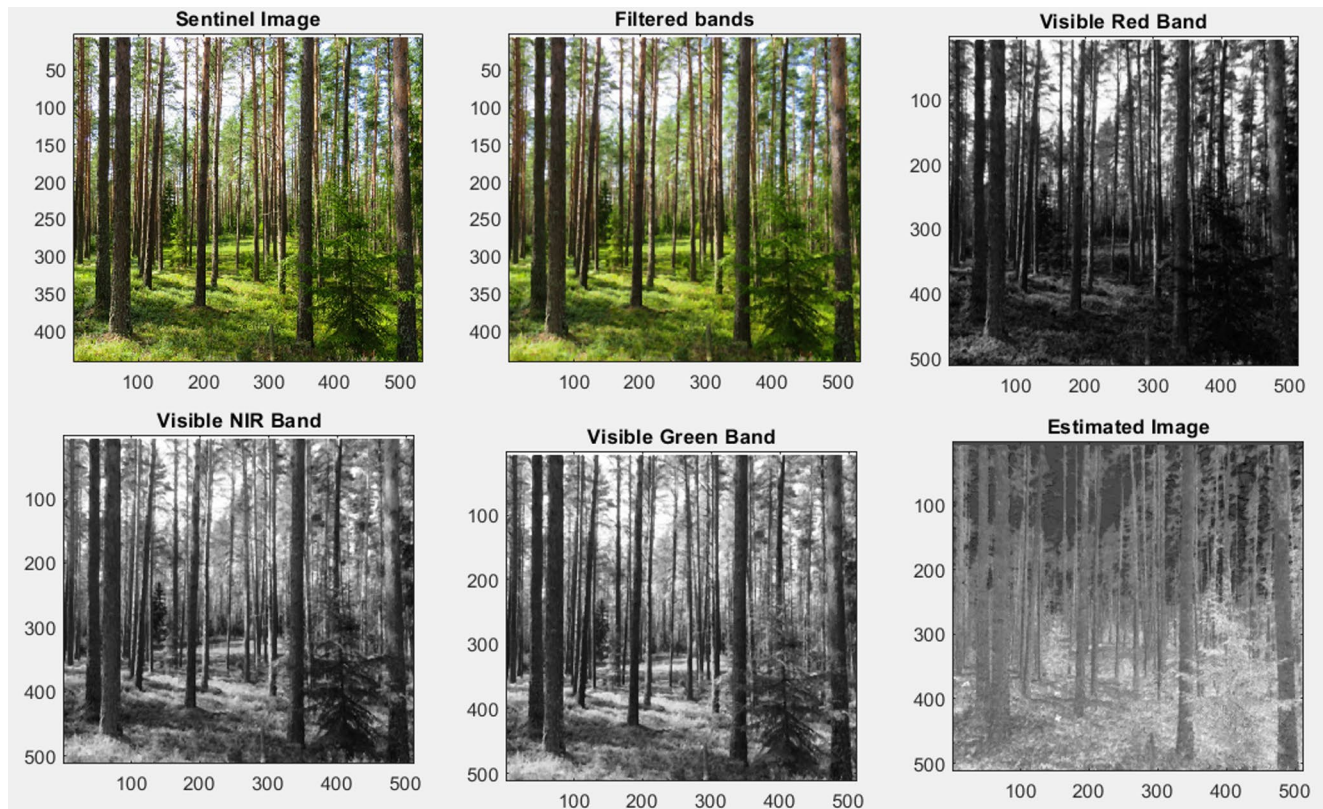


Fig. 3 Illustration of sentinel image pre-processing steps of the proposed model

phase image I^B . The input layer receives a 2D image I^B with size of 512×512 . The initial convolution layer Conv ($64, 3 \times 3$) analyzes the image I using 64 filters, each having a kernel size of 3×3 and a stride of 2. The Conv2D layer is subsequently linked to the standard BN layer. A leaky ReLU activation function is utilized to improve outcomes at each layer in place of conventional activation functions. The second convolutional layer, Conv ($128, 3 \times 3$), receives the output from the first layer's activation function and processes it using 128 filters of dimensions 3×3 , thereafter applying batch normalization and a leaky ReLU activation function. The third convolutional layer, Conv ($64, 3 \times 3$), analyses the output from the activation function of the first layer utilizing 64 filters of dimensions 3×3 , succeeded by batch normalization and leaky ReLU activation. The number of filters is increased in the second layer to extract more significant features from the sentinel image for improved classification. In the third layer, it is reduced to 64 to alleviate the problem of excessive dimensionality. Thus, the proposed layers markedly improve the precision of crop-type recognition results. The mathematical framework of the suggested CNN model is detailed below. The proposed CNN takes input and applies a unified squashing function based on the configuration of each layer, as illustrated in Eq. (7).

$$f_j^l = \left(a \left(BN \left(\sum_i y_j^{l-1} (I^B) * k_{ij} \right) + b_j^l \right) \right) \quad (7)$$

where,

- f_j^l is result of 2D CNN features extraction using convolutional layers l of j^{th} input,
- y_j^{l-1} depicts the feature mappings of the input from the preceding convolutional layer I^B ,
- k_{ij} represents i^{th} trained convolutional kernels,
- b_j^l represents the additive bias.
- $a(\cdot)$ represents the activation function,

The activation functions are layers between or after neural networks. They control neuron firing. The fundamental CNN activation function is ReLU. ReLU slows neural network computation's exponential growth. With CNN size, ReLUs increase computational cost proportionally. Since ReLU partially addresses vanishing gradients, CNN models train faster and perform better. If x is below zero, ReLU layer thresholds it to zero in Eq. (8).

$$f(x) = \begin{cases} x, & x \geq 0 \\ 0, & x < 0 \end{cases} \quad (8)$$

The leaky ReLU activation function is introduced to address the issues associated with the ReLU activation function. A leaky ReLU layer implements a threshold operation that multiplies every input value x that is less than zero by a constant scalar, as seen in Eq. (9).

$$f(x) = \begin{cases} x, & x \geq 0 \\ scale \times x, & x < 0 \end{cases} \quad (9)$$

where, $scale$ default value is set to 0.01.

BN improves neural network model performance and reliability in DL. Since it reduces internal covariate shifts, it is very useful for training large networks. BN standardizes CNN interlayer outputs via supervised learning. The next layer receives a "reset" of the output distribution from the previous layer, allowing it to assess data more effectively. The final layer of the ACNN is the flatten layer. In a CNN, the flatten layer transforms a multidimensional input into a one-dimensional array. This is executed to prepare the data for input into an artificial neural network. The flatten layer facilitates the transition from convolutional or spatially organized input to fully linked layers. The flatten layer is straightforward, and compatible, and diminishes dimensionality. Consequently, it aids in addressing the challenges associated with traditional CNN models for automated crop-type detection.

4.3 C. Classification phase

We differently designed the automatic feature learning phase (ACNN) and classification phase to effectively perform the incremental learning to acquire newly received data samples without need of re-training of entire model. The classification phase consists of L1 regularization of received ACNN feature vector, FCLs, and SoftMax classification. The incorporation of an L1 regularization layer following flatten block is a significant modification to the CNN model. Subpar DL models arise from overfitting or underfitting. Complex models, such as neural networks, are prone to overfitting training data. Consequently, regularization is essential to constrain our model and prevent overfitting to the training data. The model mitigated overfitting and underfitting by L1 regularization and feature selection. L1 regularization, referred to as the L1 norm or Lasso in regression, diminishes parameters to zero to mitigate overfitting. Certain functionalities become obsolete. This is a form of feature selection, as a weight of 0 nullifies feature values, hence diminishing their significance. Equation (10) extends the loss function to incorporate L1 regularization

$$L1 = \frac{1}{N} \sum_{i=1}^N (\hat{Y}_i - Y_i)^2 \quad (10)$$

where, N is the total number of observations, Y_i is the actual values, and \hat{Y}_i is the projected values. The revised mathematical expression for $L1$ regularization is shown below.

$$L1 = \frac{1}{N} \sum_{i=1}^N (\hat{Y}_i - Y_i)^2 + \gamma \sum_{i=1}^N |\varnothing| \quad (11)$$

where, \varnothing represents the number of observations that reduced parameters towards 0.

The subsequent step following $L1$ regularization has two fully connected layers (FCLs). Each FCL consists of biases, weights, and neurons (50 and 100), enabling connections between neurons in two separate layers. These layers usually precede the output layer and represent the last stages of a CNN architecture. The output of the second fully connected layer is inputted into the classification layer, where a SoftMax classifier is employed. The SoftMax classifier calculates the probability for each training crop type and predicts the final crop type as a consequence. The hyperparameters for each classifier are given below.

- For the SoftMax model, 10,000 epochs, 128 batches, and an Adam optimizer were used. We started with a 0.000005 learning rate and global adaption per epoch. We lowered the training cross-entropy error by 20% for the following epoch if it did not decrease after 100 (the minimum learning rate was 0.0000006).
- To achieve optimal performance with the radial basis function (RBF)-based support vector machine (RBF-SVM), we were required to optimize two hyperparameters. The kernel parameter and the penalty parameter were the kinds of hyperparameters that were affected. During the experimental inquiry, the default settings for these two hyperparameters were determined and defined.
- The major parameters of the RF model were the total number of decision trees (n_trees) to be implemented and the number of predictors that were present at each node split of the decision tree. There was a range of 200 to 5,000 for the grid search parameters for the “ n_trees ” parameter, with increments of 200.

Since the ACNN-IT uses adaptive (incremental learning), its efficacy must be objectively assessed. The data is split into 70% training and 30% testing, and we give two sub-training sample sets of 5% each. Two 5% samples were randomly selected from the 100% dataset. The remaining 90% is split 70% for training and 30% for testing. The proposed and current models used the 5% subgroups twice during the trial. To demonstrate time-series sentinel data analysis, the simulation results are reviewed for the complete dataset

after three executions (90% dataset, subsequent 5%, and final 5%).

5 Simulation results

MATLAB 2022a is used on a computer running Windows 11 that has 8 gigabytes of random-access memory (RAM) and an Intel i5 processor. The use of MATLAB for simulation studies is a frequent practice, particularly for those studies that entail the processing of multimedia data. It has been established that the statistics of the dataset, in addition to the list of hyperparameters, have been discussed in an earlier section of this study. For crop-type mapping, the ACNN-IT model was put through a comparative analysis with three conventional machine learning techniques: SoftMax, SVM, and RF. Five metrics were applied, and they were as follows: overall accuracy (OA), precision (P), recall (R), specificity (S), and F1-score (F1). Equation (12) to (16) were utilized to achieve the determination of these measures. With the assistance of Operational Analytics (OA), the performance of different models for crop-type classification was examined. The F1 score was then applied to find the most appropriate date for the detection of each crop type during the growing season. The following is a list of the formulas that are associated with the relevant computations:

$$OA = \frac{(TP + TN)}{(TP + FP + TN + FN)} \quad (12)$$

$$S = \frac{TN}{(TN + FP)} \quad (13)$$

$$R = \frac{TP}{(TP + FN)} \quad (14)$$

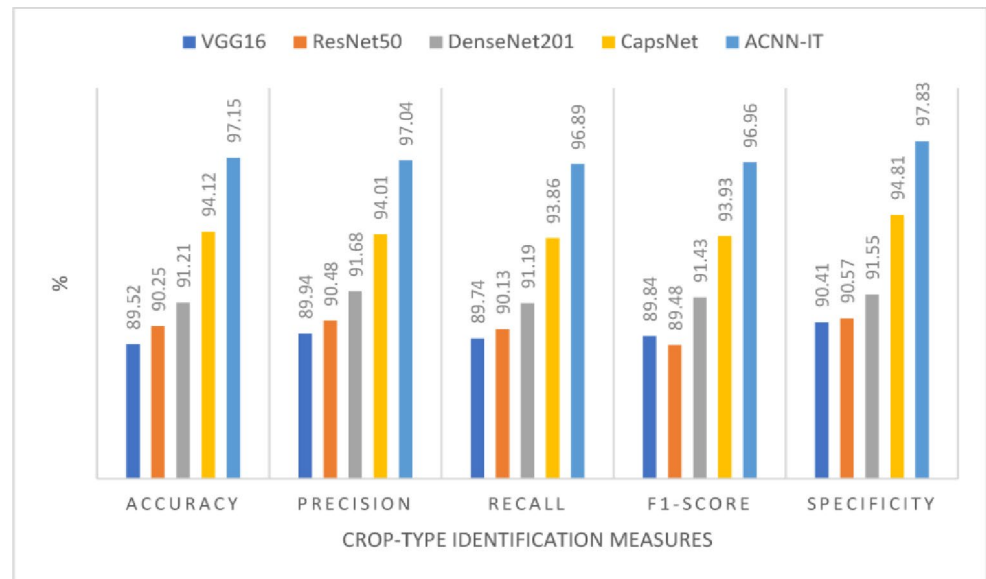
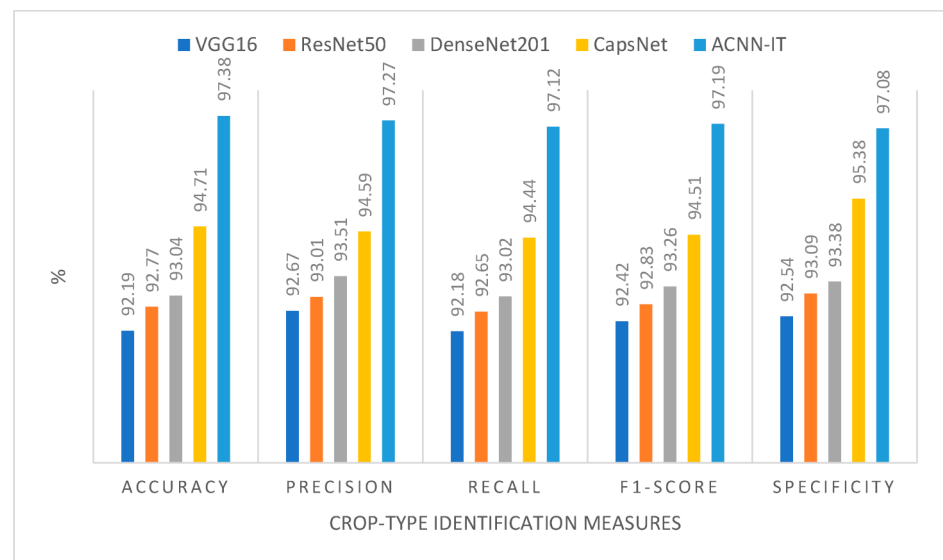
$$P = \frac{TP}{(TP + FP)} \quad (15)$$

$$F1 = \frac{2TP}{(2TP + FP + FN)} \quad (16)$$

To evaluate the proposed automated crop-type categorization, we make use of the performance measures of True Positive (TP), True Negative (TN), False Positive (FP), and False Negative (FN).

5.1 A. ACNN-IT analysis

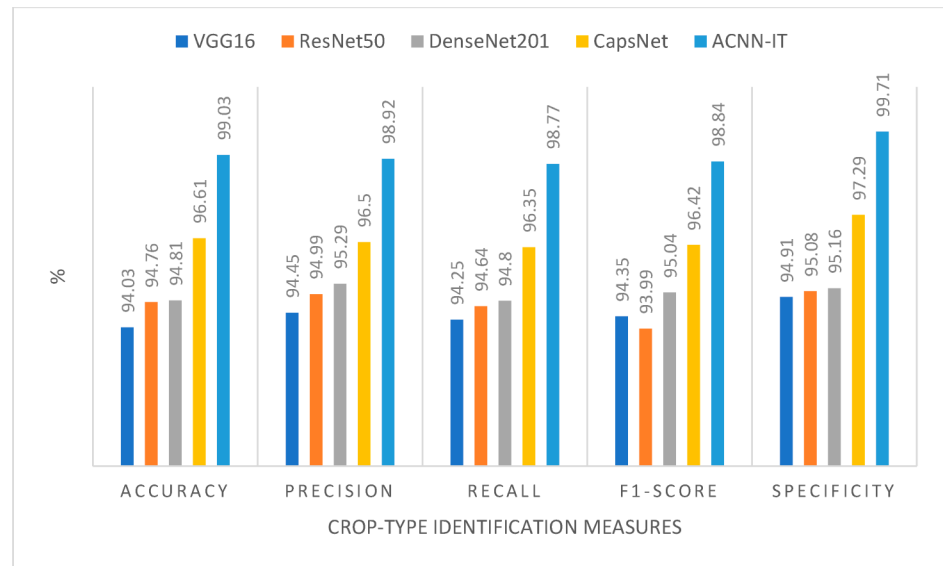
This section presents the performance analysis of early in-season crop-type detection using the ACNN-IT model. As three different classifiers were used, this section presents

Fig. 4 Crop-type identification analysis using SVM classifier**Fig. 5** Crop-type identification analysis using RF classifier

the comparative analysis among different DL models with ACNN-IT model using SVM, RF, and SoftMax classifiers in terms of OA, P, R, S, and F1 measures. Figures 4, 5 and 6 show the early automatic crop-type detection using existing DL models such as VGG16 [53], ResNet50 [54], DenseNet201 [55], and CapsNet [56]. The proposed ACNN-IT model is compared with these recently introduced CNN models to verify the early crop-type identification efficiency.

As shown in Figs. 3, 4 and 5, the proposed ACNN-IT approach has improved the overall performances compared to other DL models for automatic early in-season crop-type identification. As discussed earlier, the above results are an average of three consecutive executions using the input time-series dataset. Each model is trained for newly acquired 5% sentinel data samples, and re-evaluations were performed. Figures show the average results for each of the

DL models using three different classifiers. The ACNN-IT shows the improved in-season crop-type identification outcomes using each classifier compared to all DL models. The OA and F1 using the SVM classifier for ACNN-IT are 97.15% and 96.96% which is way ahead of the second-best DL method CapsNet (OA-94.12 and F1-93.93). The OA and F1 scores for the RF classifier applied to ACNN-IT are 97.38% and 97.19%, respectively, significantly surpassing the second-best DL approach, CapsNet, which has an OA of 94.71% and an F1 score of 94.51%. Finally, the OA and F1 score for the SoftMax classifier applied to ACNN-IT are 99.03% and 98.84%, respectively, markedly exceeding the second-best deep learning method, CapsNet, which has an OA of 96.61% and an F1 score of 96.42%. The influence of OA and F1 metrics directly affects other classification measures' precision, recall, and specificity. Consequently, it

Fig. 6 Crop-type identification analysis using SoftMax classifier**Table 3** Comparative analysis of AET

| DL Methods | AET (minutes) |
|-------------|---------------|
| VGG16 | 572.42 |
| ResNet50 | 546.23 |
| DenseNet201 | 528.93 |
| CapsNet | 489.23 |
| ACNN-IT | 339.42 |

Table 4 Crop-type identification analysis using different classifiers

| Measures | SVM | RF | SoftMax |
|-------------|-------|-------|---------|
| Accuracy | 97.15 | 97.38 | 99.03 |
| Precision | 97.04 | 97.27 | 98.92 |
| Recall | 96.89 | 97.12 | 98.77 |
| F1-score | 96.96 | 97.19 | 98.84 |
| Specificity | 97.83 | 97.08 | 99.71 |

exhibits a comparable performance pattern to the OA and F1 metrics. The principal factors contributing to the performance enhancement of the ACNN-IT model with various classifiers are elaborated upon thereafter. Initially, ACNN-IT has proficiently pre-processed the obtained sentinel pictures to enhance feature estimation using a hybrid approach of coefficient computation (NDVI combined with backscattering analysis). Current methodologies lack this technique, resulting in diminished accuracy in crop-type detection. Secondly, ACNN layers are structured in two phases: automated feature learning and classification, enabling them to readily adapt to freshly obtained time-series sentinel data. The ACNN-IT model incorporates an incremental learning strategy, a feature absent in current deep learning models. Consequently, it impacts the overall classification performance. The modified CNN layers in the ACNN approach have also addressed the problems of high feature dimensions, overfitting, and exploding gradients. Adaptability of the proposed model also results into lower computational efforts Average Execution Time (AET) compared to existing DL models as showing in Table 3. These problems are associated with existing methods and hence result in less efficiency compared to the ACNN-IT approach.

5.2 B. ablation study

In this section, we investigate the different factors that we have utilized in ACNN-IT model to perform ablation study such as classifiers analysis (SVM, RF, and SoftMax), then impact of L1 regularization, and impact of leaky ReLU activation function. Table 4 shows that crop-type identification analysis using different classifiers in ACNN-IT model. As showing in Table 4, SoftMax classifier has delivered the best performances over the conventional ML classifiers. The classification efficiency of the SoftMax is approximately 2+ % compared to both SVM and RF classifiers. The Softmax function is extensively utilized for multi-class classification tasks, when an instance may belong to one of several potential classes. It offers a method to assign probabilities to each class, hence assisting in determining the most probable class for a given input instance.

Table 5 shows how regularization affects the proposed model. Using L1 regularization improves performance by about 3%. It justified the influence of L1 regularization before FCLs in the suggested paradigm. In-season crop-type identification efficiency is also improved. CNN regularization improves generalization, model robustness, overfitting risk, and test accuracy. It can simplify the model, save computation costs, and increase explainability and interpretability. Finally, Table 6 shows how the Leaky ReLU activation

Table 5 Crop-type identification analysis using regularization

| Measures | Without Regularization | With Regularization |
|-------------|------------------------|---------------------|
| Accuracy | 96.67 | 99.03 |
| Precision | 96.56 | 98.92 |
| Recall | 96.41 | 98.77 |
| F1-score | 96.48 | 98.84 |
| Specificity | 97.35 | 99.71 |

Table 6 Crop-type identification analysis using activation function

| Measures | Sigmoid | ReLU | Leaky ReLU |
|-------------|---------|-------|------------|
| Accuracy | 96.59 | 96.82 | 99.03 |
| Precision | 96.48 | 96.71 | 98.92 |
| Recall | 96.33 | 96.56 | 98.77 |
| F1-score | 96.4 | 96.63 | 98.84 |
| Specificity | 97.27 | 96.52 | 99.71 |

Table 7 Comparative analysis with existing methods using Adam optimizer

| Methods | OA | AET (minutes) |
|---------|-------|---------------|
| [36] | 87.82 | 563.33 |
| [39] | 91.23 | 498.89 |
| [42] | 94.38 | 578.23 |
| [43] | 93.71 | 547.45 |
| [44] | 92.45 | 539.1 |
| [45] | 93.82 | 582.3 |
| [46] | 94.21 | 489.62 |
| [47] | 93.56 | 478.23 |
| [48] | 94.03 | 511.47 |
| ACNN-IT | 99.03 | 339.42 |

Table 8 Comparative analysis with existing methods using SGD optimizer

| Methods | OA | AET (minutes) |
|---------|-------|---------------|
| [36] | 86.73 | 532.1 |
| [39] | 90.14 | 467.66 |
| [42] | 93.29 | 547 |
| [43] | 92.62 | 516.22 |
| [44] | 91.36 | 507.87 |
| [45] | 92.73 | 551.07 |
| [46] | 93.12 | 458.39 |
| [47] | 92.47 | 447 |
| [48] | 92.94 | 480.24 |
| ACNN-IT | 97.94 | 308.19 |

function affects the proposed model. It reveals that the Leaky ReLU activation function is more efficient than the other two. The Vanishing Gradient Problem is solved with leaky ReLU. Leaky ReLU eases Dying ReLU.

5.3 C. state-of-the-arts analysis

This study concludes with a comparison of contemporary crop-type analysis algorithms utilizing the input data. The comparative study focuses on OA and average execution time. Table 7 shows the comparative analysis of the



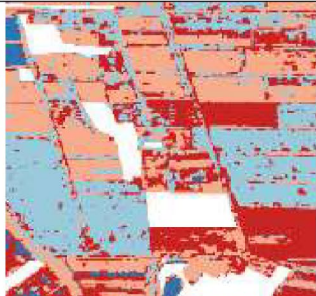


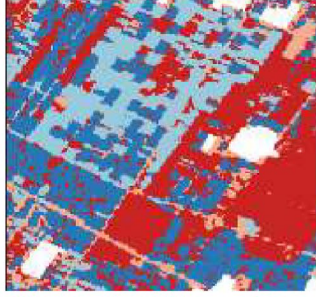
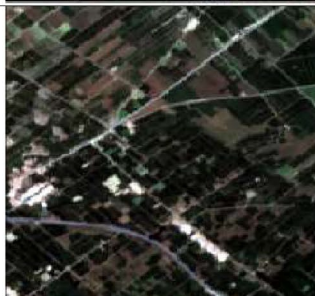
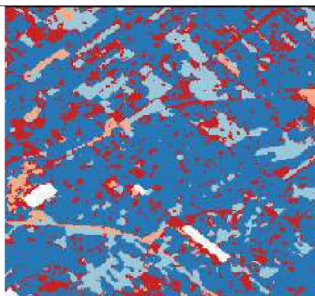
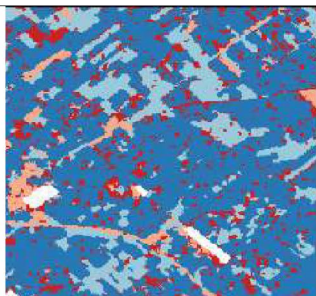

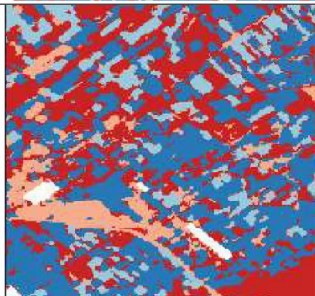

proposed model with total 9 existing methods from [36, 39], and [42–48]. For these methods Adam optimizer was used. Table 8 shows the comparative analysis of the proposed model using Stochastic Gradient Descent (SGD) optimizer. These nine existing DL techniques for crop-type identification were chosen for comparison with the proposed model. These approaches employ the same setups as our suggested model. The results in Tables 7 and 8 reveals that the proposed model outperforms existing techniques in-season crop-type detection for OA and AET. The primary factors that increase ACNN-IT model performance with different classifiers are listed below. Through NDVI and backscattering analysis, ACNN-IT accurately pre-processed sentinel images to improve feature estimation. This approach is missing, limiting crop-type identification accuracy. Automatic feature learning and categorization allow ACNN layers to respond to fresh time-series sentinel data. The ACNN-IT model employs incremental learning, unlike standard deep learning. Thus, AET and OA classification performance is affected. ACNN's enhanced CNN layers manage overfitting, high-size features, and explosive gradients. These drawbacks make existing methods less efficient than ACNN-IT.

Among Existing methods, the method proposed in [42] delivered the second-best crop classification results. Table 9 presents the visual findings for four agricultural zones in the Pune district. The outcomes for crop categorization demonstrate a comparison between the suggested technique and the recently introduced method in [42]. As the method in [42] delivered the optimum classification accuracy compared to other existing methods, we have selected it for the visual analysis in Table 9. The chosen agricultural zones encompass several crops, including forest, corn, cotton, fruit trees, and CYR. The categorization results illustrate the mapping of these crops utilizing various colors. The visual outcome shows that the proposed model classifies some crop regions with complete colors compared to the existing approach. The suggested model enhances classification results for the reasons previously stated.

6 Conclusion

This work offered a unique technique for crop type detection utilizing the ACNN-IT model with time-series data from Sentinel-1 A and Sentinel-2. The proposed model was evaluated on a real-time dataset collected from the Pune (India) region. The gathered data is initially processed to transform it into image format. The received sentinel images were then pre-processed for quality improvement and hybrid coefficient estimation. It helped to improve the feature engineering for crop-type identification. The adaptive DL layers are

Table 9 Visual outcomes for crop classification using proposed and existing methods

| Input Crop Area | Existing Crop-mapping Classification | Proposed Crop-mapping Classification |
|---|---|--|
|  |  |  |
|  |  |  |
|  |  |  |
|  |  |  |

designed for automatic feature estimation from the pre-processed sentinel image. The adaptive and lightweight CNN layers gradually learn time-series sentinel data, improving early season information use and optical and radar data sensitivities across various parameters. As the CNN layers are designed with an incremental learning approach, it takes very little time to train newly acquired sentinel data. It also results in improved overall accuracy. The classification phase was designed for appropriate crop-type mapping using the FCLs and SoftMax classifier. Simulation results revealed that the proposed model significantly improved

the in-season crop-type mapping performances compared to recently proposed similar methods. The overall accuracy of the proposed model is improved by 7.32% and processing time is reduced by 34.56% compared to existing methods. Introducing AI algorithms for feature selection will be the vital research direction to improve the proposed model in future work.

Funding No funding.

Data availability The datasets analysed during the current study are available from the corresponding author on reasonable request.

Declarations

Conflict of interest All authors declares that they has no conflict of interest.

Ethical approval This article does not contain any studies with human participants performed by any of the authors.

References

- Beriaux E, Jago A, Lucau-Danila C, Planchon V, Defourny P (2021) Sentinel-1 time series for crop identification in the framework of the future CAP monitoring. *Remote Sens* 13(14):2785. <https://doi.org/10.3390/rs13142785>
- Tomppo E, Antropov O, Praks J (2019) Cropland classification using Sentinel-1 time series: methodological performance and prediction uncertainty assessment. *Remote Sens* 11(21):2480. <https://doi.org/10.3390/rs11212480>
- Xie Q, Lai K, Wang J, Lopez-Sanchez JM, Shang J, Liao C, Zhu J, Fu H, Peng X (2021) Crop monitoring and classification using polarimetric RADARSAT-2 Time-Series data across growing season: A case study in Southwestern Ontario, Canada. *Remote Sens* 13(7):1394. <https://doi.org/10.3390/rs13071394>
- Xie Y, Huang J (2021) Integration of a crop growth model and deep learning methods to improve Satellite-Based yield Estimation of winter wheat in Henan Province, China. *Remote Sens* 13(21):4372. <https://doi.org/10.3390/rs13214372>
- Jiang H, Li D, Jing W, Xu J, Huang J, Yang J, Chen S (2019) Early season mapping of sugarcane by applying machine learning algorithms to Sentinel-1A/2 time series data: A case study in Zhanjiang City, China. 11(7):861–861. <https://doi.org/10.3390/rs11070861>
- Dey S, Bhogapurapu N, Homayouni S, Bhattacharya A, McNairn H (2021) Unsupervised classification of crop growth stages with scattering parameters from Dual-Pol Sentinel-1 SAR data. *Remote Sens* 13(21):4412. <https://doi.org/10.3390/rs13214412>
- Wei M, Qiao B, Zhao J, Zuo X (2019) The area extraction of winter wheat in mixed planting area based on Sentinel-2 a remote sensing satellite images. 35(3):297–308. <https://doi.org/10.1080/17445760.2019.1597084>
- Desai GT, Gaikwad AN (2022) Automatic land cover classification with SAR imagery and machine learning using Google Earth engine. *Int J Electr Comput Eng Syst* 13(10):909–916. <https://doi.org/10.32985/ijeces.13.10.6>
- Pan L, Xia H, Zhao X, Guo Y, Qin Y (2021) Mapping winter crops using a phenology algorithm, Time-Series Sentinel-2 and Landsat-7/8 images, and Google Earth engine. *Remote Sens* 13(13):2510. <https://doi.org/10.3390/rs13132510>
- Busquier M, Valcarce-Diñeiro R, Lopez-Sanchez JM, Plaza J, Sánchez N, Arias-Pérez B (2021) Fusion of Multi-Temporal PAZ and Sentinel-1 data for crop classification. *Remote Sens* 13(19):3915. <https://doi.org/10.3390/rs13193915>
- Luo C, Qi B, Liu H, Guo D, Lu L, Fu Q, Shao Y (2021) Using time series Sentinel-1 images for Object-Oriented crop classification in Google Earth engine. *Remote Sens* 13(4):561. <https://doi.org/10.3390/rs13040561>
- Canisius F, Shang J, Liu J, Huang X, Ma B, Jiao X, Geng X, Kovacs JM, Walters D (2018) Tracking crop phenological development using multi-temporal polarimetric Radarsat-2 data. *Remote Sens Environ* 210:508–518. <https://doi.org/10.1016/j.rse.2017.07.031>
- Kaushik SK, Mishra VN, Punia M et al (2021) Crop health assessment using Sentinel-1 SAR time series data in a part of central India. *Remote Sens Earth Syst Sci* 4:217–234. <https://doi.org/10.1007/s41976-021-00064-z>
- Kolotii A, Kussul N, Shelestov A, Skakun S, Yailymov B, Basarab R, Lavreniuk M, Oliynyk T, Ostapenko V (2015) Comparison of biophysical and satellite predictors for wheat yield forecasting in Ukraine. *ISPRS - Int Archives Photogrammetry Remote Sens Spat Inform Sci XL-7/W3:39–44*. <https://doi.org/10.5194/isprsarchives-xl-7-w3-39-2015>
- Cai Y, Guan K, Peng J, Wang S, Seifert C, Wardlow B, Li Z (2018) A high-performance and in-season classification system of field-level crop types using time-series Landsat data and a machine learning approach. *Remote Sens Environ* 210:35–47. <https://doi.org/10.1016/j.rse.2018.02.045>
- Kobayashi N, Tani H, Wang X, Sonobe R (2019) Crop classification using spectral indices derived from Sentinel-2A imagery. *J Inform Telecommunication* 1–24. <https://doi.org/10.1080/24751839.2019.1694765>
- Vreugdenhil M, Wagner W, Bauer-Marschallinger B, Pfeil I, Teubner I, Rüdiger C, Strauss P (2018) Sensitivity of Sentinel-1 backscatter to vegetation dynamics: an Austrian case study. *Remote Sens* 10(9):1396. <https://doi.org/10.3390/rs10091396>
- Ndikumana E, Ho Tong Minh D, Baghdadi N, Courault D, Hosard L (2018) Deep recurrent neural network for agricultural classification using multitemporal SAR Sentinel-1 for Camargue, France. *Remote Sens* 10(8):1217. <https://doi.org/10.3390/rs10081217>
- Yuan Q, Shen H, Li T, Li Z, Li S, Jiang Y, Xu H, Tan W, Yang Q, Wang J, Gao J, Zhang L (2020) Deep learning in environmental remote sensing: achievements and challenges. *Remote Sens Environ* 241:111716. <https://doi.org/10.1016/j.rse.2020.111716>
- Ismail Fawaz H, Forestier G, Weber J et al (2019) Deep learning for time series classification: a review. *Data Min Knowl Disc* 33:917–963. <https://doi.org/10.1007/s10618-019-00619-1>
- Liao C, Wang J, Xie Q, Baz AA, Huang X, Shang J, He Y (2020) Synergistic use of Multi-Temporal RADARSAT-2 and VENUS data for crop classification based on 1D convolutional neural network. *Remote Sens* 12(5):832. <https://doi.org/10.3390/rs12050832>
- Zhao W, Qu Y, Chen J, Yuan Z (2020) Deeply synergistic optical and SAR time series for crop dynamic monitoring. *Remote Sens Environ* 247:111952. <https://doi.org/10.1016/j.rse.2020.111952>
- Hegazi EH, Yang L, Huang J (2021) A convolutional neural network algorithm for soil moisture prediction from Sentinel-1 SAR images. *Remote Sens* 13(24):4964. <https://doi.org/10.3390/rs13244964>
- Liu J, Xu Y, Li H, Guo J (2021) Soil moisture retrieval in farmland areas with Sentinel Multi-Source data based on regression convolutional neural networks. 21(3):877–877. <https://doi.org/10.3390/s21030877>
- Efremova N, Seddik ME Amine, Erten E (2022) Soil moisture Estimation using Sentinel-1/-2 imagery coupled with cyclegan for Time-Series gap filing. *IEEE Trans Geosci Remote Sens* 60:4705111. <https://doi.org/10.1109/TGRS.2021.3134127>
- Habiboullah A, Louly MA (2022) Soil moisture prediction based on satellite data using a novel deep learning model. *Commun Comput Inform Sci* 394–408. https://doi.org/10.1007/978-3-031-08277-1_32
- Mehmet Furkan Çelik MS, Işık O, Yüzügüllü N, Esra Erten (2022) Soil moisture prediction from remote sensing images coupled with climate, soil texture and topography via deep learning. *Remote Sens* 14(21):5584–5584. <https://doi.org/10.3390/rs14215584>
- Singh A, Gaurav K (2023) Deep learning and data fusion to estimate surface soil moisture from multi-sensor satellite images. *Sci Rep* 13(1). <https://doi.org/10.1038/s41598-023-28939-9>

29. Dabboor M, Atteia G, Meshoul S, Alayed W (2023) Deep Learning-Based framework for soil moisture content retrieval of bare soil from satellite data. *Remote Sens* 15(7):1916. <https://doi.org/10.3390/rs15071916>
30. Nijaguna GS, Manjunath DR, Abouhawwash M, Askar SS, Basha DK, Sengupta J (2023) Deep Learning-Based improved WCM technique for soil moisture retrieval with satellite images. *Remote Sens* 15(8):2005. <https://doi.org/10.3390/rs15082005>
31. Vishal Batchu, Nearing G, Varun Gulshan (2023) SoilGrids, SMAP-USDA, and GLDAS for Soil Moisture Retrieval. *J Hydrometeorol* 24(10):1789–1823. <https://doi.org/10.1175/jhm-d-22-0118.1>
32. Hegazi EH, Samak AA, Yang L, Huang R, Huang J (2023) Prediction of soil moisture content from Sentinel-2 images using convolutional neural network (CNN). *Agronomy* 13(3):656. <https://doi.org/10.3390/agronomy13030656>
33. Zhu L, Dai J, Liu Y, Yuan S, Qin T, Walker JP (2024) A cross-resolution transfer learning approach for soil moisture retrieval from Sentinel-1 using limited training samples. *Remote Sens Environ* 301:113944. <https://doi.org/10.1016/j.rse.2023.113944>
34. Rivera Rivas A, Pérez-Godoy M, Elizondo D, Deka, Lipika, Del Jesus, María José (2022) Analysis of clustering methods for crop type mapping using satellite imagery. *Neurocomputing* 492. <https://doi.org/10.1016/j.neucom.2022.04.002>
35. Guo Z, Qi W, Huang Y, Zhao J, Yang H, Koo V-C, Li N (2022) Identification of crop type based on C-AENN using time series Sentinel-1A SAR data. *Remote Sens* 14(6):1379. <https://doi.org/10.3390/rs14061379>
36. Mao M, Zhao H, Tang G, Ren J (2023) In-Season crop type detection by combining Sentinel-1A and Sentinel-2 imagery based on the CNN model. *Agronomy* 13:1723. <https://doi.org/10.3390/agronomy13071723>
37. Wang Y, Huang H, State R (2023) Early crop mapping using dynamic ecoregion clustering: A USA-Wide study. *Remote Sens* 15:4962. <https://doi.org/10.3390/rs15204962>
38. Alami Machichi, M., mansouri, loubna E., imani, yasmina, Bourja, O., Lahlou, O., Zennayi, Y., ... Hadria, R. (2023). Crop mapping using supervised machine learning and deep learning: a systematic literature review. *International Journal of Remote Sensing*, 44(8), 2717–2753. <https://doi.org/10.1080/01431161.2023.2205984>
39. Ayushi, Buttar P (2024) Satellite imagery analysis for crop type segmentation using U- net architecture. *Procedia Comput Sci* 235. <https://doi.org/10.1016/j.procs.2024.04.322>
40. Mohammadi S, Belgiu M, Stein A (2024) Few-Shot learning for crop mapping from satellite image time series. *Remote Sens* 16:1026. <https://doi.org/10.3390/rs16061026>
41. Kaijage B, Belgiu M, Bijker W (2024) Spatially explicit active learning for Crop-Type mapping from satellite image time series. *Sensors* 24(7):2108. <https://doi.org/10.3390/s24072108>
42. Teimouri M, Mokhtarzade M, Baghdadi N et al (2023) Generating Virtual Training Labels for Crop Classification from Fused Sentinel-1 and Sentinel-2 Time Series. *PFG* 91, 413–423 <https://doi.org/10.1007/s41064-023-00256-w>
43. Antonijević O, Jelić S, Bajat B et al (2023) Transfer learning approach based on satellite image time series for the crop classification problem. *J Big Data* 10:54. <https://doi.org/10.1186/s40537-023-00735-2>
44. Song, Weicheng & Feng, Aiqing & Wang, Guojie & Zhang, Qixia & Dai, Wen & Wei, Xikun & Hu, Yifan & Amankwah, Solomon & Zhou, Feihong & Liu, Yi. (2023). Bi-Objective Crop Mapping from Sentinel-2 Images Based on Multiple Deep Learning Networks. *Remote Sensing*. 15. 3417. [10.3390/rs15133417](https://doi.org/10.3390/rs15133417).
45. Ahmed B, Akram T, Naqvi SR, Alsuhaibani A, Altherwy YN, Masud U (2024) A novel deep learning framework with Meta-Heuristic feature selection for enhanced remote sensing image classification. *IEEE Access* 12:91974–91998. <https://doi.org/10.1109/access.2024.3422368>
46. Li X, Xie L, Wang C, Miao J, Shen H, Zhang L (2024) Boundary-enhanced dual-stream network for semantic segmentation of high-resolution remote sensing images. *GIScience Remote Sens* 61(1). <https://doi.org/10.1080/15481603.2024.2356355>
47. Eisfelder C, Boemke B, Gessner U, Sogno P, Alemu G, Hailu R, Mesmer C, Huth J (2024) Cropland and crop type classification with Sentinel-1 and Sentinel-2 time series using Google Earth engine for agricultural monitoring in Ethiopia. *Remote Sens* 16(5):866. <https://doi.org/10.3390/rs16050866>
48. Barriere V, Claverie M, Schneider M, Lemoine G, d'Andrimont R (2024) Boosting crop classification by hierarchically fusing satellite, rotational, and contextual data. *Remote Sens Environ* 305:114110. <https://doi.org/10.1016/j.rse.2024.114110>
49. Zheng Y, Dong W, Lu Y, Zhang X, Dong Y, Sun F (2024) A new attention-based deep metric model for crop type mapping in complex agricultural landscapes using multisource remote sensing data. *Int J Appl Earth Obs Geoinf* 134:104204. <https://doi.org/10.1016/j.jag.2024.104204>
50. Xue H, Fan Y, Dong G, He S, Lian Y, Luan W (2024) Crop classification in the middle reaches of the Hei river based on model transfer. *Sci Rep* 14(1). <https://doi.org/10.1038/s41598-024-80327-z>
51. Altun M, Turker M (2025) Integration of convolutional neural networks with parcel-based image analysis for crop type mapping from time-series images. *Earth Sci Inf* 18(3). <https://doi.org/10.1007/s12145-025-01819-8>
52. Muñoz D, Narváez C, Cobos C, Mendoza M, Herrera F (2020) Incremental learning model inspired in rehearsal for deep convolutional networks. *Knowl Based Syst* 208:106460. <https://doi.org/10.1016/j.knosys.2020.106460>
53. Veni N, Manjula J (2023) VGG-16 architecture for MRI brain tumor image classification. In: Subhashini N, Ezra MAG, Liaw SK (eds) *Futuristic communication and network technologies. Lecture Notes in Electrical Engineering*, vol 966. Springer, Singapore. https://doi.org/10.1007/978-981-19-8338-2_26
54. Krichen M (2023) Convolutional neural networks: A survey. *Computers* 12(8):151–151. <https://doi.org/10.3390/computers12080151>
55. Hasan N, Bao Y, Shawon A et al (2021) DenseNet convolutional neural networks application for predicting COVID-19 using CT image. *SN COMPUT SCI* 2:389. <https://doi.org/10.1007/s42979-021-00782-7>
56. Marjit Singh M, Kumar Sarkar N (2024) Capsule network approach for image classification. *Lecture Notes Networks Syst* 639–649. https://doi.org/10.1007/978-981-99-9442-7_53

Publisher's note Springer Nature remains neutral with regard to jurisdictional claims in published maps and institutional affiliations.

Springer Nature or its licensor (e.g. a society or other partner) holds exclusive rights to this article under a publishing agreement with the author(s) or other rightsholder(s); author self-archiving of the accepted manuscript version of this article is solely governed by the terms of such publishing agreement and applicable law.